Time-dependent configuration-interaction calculations of laser-pulse-driven many-electron dynamics: Controlled dipole switching in lithium cyanide

Pascal Krause, Tillmann Klamroth,[a] and Peter Saalfrank
Theoretische Chemie, Institut für Chemie, Universität Potsdam, Karl-Liebknecht-Straße 24-25, D-14476 Potsdam, Germany

(Received 20 April 2005; accepted 14 June 2005; published online 23 August 2005)

We report simulations of laser-driven many-electron dynamics by means of the time-dependent configuration interaction singles (doubles) approach. The method accounts for the correlation of ground and excited states, is capable of describing explicitly time-dependent, nonlinear phenomena, and is systematically improvable. Lithium cyanide serves as a molecular test system in which the charge distribution and hence the dipole moment are shown to be switchable, in a controlled fashion, by (a series of) laser pulses which induce selective, state-to-state electronic transitions. One focus of our time-dependent calculations is the question of how fast the transition from the ionic ground state to a specific excited state that is embedded in a multitude of other states can be made, without creating an electronic wave packet. © *2005 American Institute of Physics*.
[DOI: 10.1063/1.1999636]

I. INTRODUCTION

The manipulation and control of single molecules are important topics for the construction of even smaller electronic devices. In the field of molecular electronics,[1,2] the ultimate goal is to construct such devices, e.g., transistors or switches, consisting of single molecules. A single molecule has not only the advantage of a small length scale in the order of a nanometer, but also of being transferable from one state to another in a very short time. For a comprehensive overview of the different time scales for ultrafast processes in chemistry, see, for example, Ref. 3. While the typical time scale for conformational changes, i.e., the rearrangement of the nuclei, is in the order of a few hundred femtoseconds, electronic transitions, such as charge transfer, can take place much faster, in a few femtoseconds (10^{-15} s) or even in the attosecond (10^{-18} s) regime.[4] Recent developments in pump-probe-laser experiments[5] have shown that one can monitor the electron dynamics with a subfemtosecond resolution. Given the parallel, impressive advances in laser technology, including the measurement of the phase between the carrier and the pulse envelope of a few-cycle laser pulse,[6–8] it seems therefore also not out of reach to control the electronic state of a molecule within time intervals as short as femtoseconds. Of course one would like to control these transitions in a state-specific manner, reversibly, and without any unwanted inter- and intramolecular side reactions.

In this paper we present explicitly time-dependent *ab initio* calculations for the laser-driven many-electron dynamics of a small molecule, i.e., lithium cyanide (LiCN). This molecule serves as a test system for light-induced charge transfer, as we investigate the dynamics of the laser-driven transition from the ionic ground state (Li^+CN^-) to a covalent excited state ($LiCN^\star$). These two states can be clearly distinguished by their permanent dipole moments along the molecular axis. It is also expected that such a dipole moment change will be accompanied by a change in other physical properties, such as the conductivity of the molecule when thought of as being part of a molecular device. On the other hand, it must also be expected that such a large change of the dipole will lead to nuclear rearrangement. In fact, some of the covalent target states we are considering below are repulsive along the Li–C bond. In this exploratory study, however, and on short enough time scales, in general, nuclear motion can be neglected as a first approximation, but should be included later on (see below).

Still, the treatment of many-electron dynamics is a computational challenge by itself. An exact solution of the time-dependent Schrödinger equation is only feasible for small systems containing a few electrons, e.g., molecules such as H_2 (Ref. 9) or simple atoms such as Be.[10] For an approximate solution one can employ the time-dependent analogs of the methods used in electronic structure theory. Two of the most well known are probably the time-dependent Hartree-Fock[11] (TD-HF) and the (explicitly) time-dependent density-functional theory (TD-DFT).[12] The TD-DFT has been widely used, for example, for laser-driven electron dynamics in metal clusters.[13] Also small molecules such as LiCN were already subjected to a TD-DFT-based simulation including the motion of the ion cores in a classical description; see, for example, Ref. 14. Both TD-HF and TD-DFT are one-determinant approaches, but while TD-DFT treats electron correlation via an (mostly semiempirical) exchange-correlation functional, in TD-HF electron correlation is missing altogether. On the way towards correlated, many-determinant methods, recently the time-dependent configuration-interaction (TD-CI) method, e.g., with single excitations (TD-CIS) was suggested[15,16] and applied to one-

[a]Electronic mail: klamroth@rz.uni-potsdam.de

dimensional model problems. Also, a time-dependent analog of the complete active space self-consistent-field (CASSCF) method,[17] also termed the multiconfiguration time-dependent Hartree-Fock (MCTDHF) method, was proposed.[18–20] The MCTDHF method is an adaption of the multiconfiguration time-dependent Hartree,[21] (MCTDH) method for fermions.

In this paper we want to present time-dependent configuration-interaction singles (doubles) [TD-CIS(D)] calculations based on the CIS(D) method of electronic structure theory.[22,23] The configuration-interaction singles (CIS) approach[24] itself is a well-established tool in quantum chemistry for an approximate calculation of excited states employing singly excited Slater determinants derived from the HF ground-state determinant. CIS is useful in cases when excited states are not dominated by double and higher excitations. The method even includes some electron correlation in the excited-state manifold, while the ground-state energy is still given by the HF energy. In CIS(D), one includes the double excitations by perturbative corrections to the ground- and excited-state energies. In this method the ground-state energy is equal to the second-order Møller-Plesset (MP2) energy,[25] i.e., the ground-state energy also includes electron correlation. The excited states are corrected as well.

The method will be applied in this work to the laser-induced charge transfer, i.e., dipole switching, of the LiCN molecule. Ultrafast laser pulses or pulse sequences are used to switch from the ionic ground state to a selected covalent state, and from there to the ground state again or to some other state. It is shown that by the proper choice of laser parameters the transitions can be made state selective, despite the target states being embedded in a multitude of neighboring electronic states. By the procedure, the dipole moment can be controlled systematically. With very short pulses, however, an electronic wave packet is created and much of the selectivity is lost.

The paper is organized as follows. In Sec. II we introduce the TD-CIS(D) approach. In Sec. III we present the results for the LiCN system. First, in Sec. III A we will briefly describe the time-independent results obtained from stationary quantum chemistry calculations. Section III B gives the results of our time-dependent calculations and Sec. III C discusses some possibilities to control the light-induced charge transfer in the molecule or dipole switching. Section IV summarizes the paper and gives an outlook for future work. We use a.u. throughout, if not stated otherwise.

II. THEORY

A. CIS(D)

The starting point for the CIS(D) calculations is the restricted Hartree-Fock ground-state Slater determinant

$$|\Psi_0^{\mathrm{HF}}\rangle = \frac{1}{\sqrt{N!}}|(\psi_1\alpha),(\psi_1\beta),\ldots,(\psi_{N/2}\alpha),(\psi_{N/2}\beta)\rangle. \tag{1}$$

Here, each of the first $N/2$ spatial molecular orbitals (MOs) ψ_i is occupied with two electrons, one with α spin and one with β spin; N being the total number of electrons. The occupied and unoccupied spatial MOs, are obtained by solving the spin- and field-free restricted Hartree-Fock equations

$$\left[-\frac{1}{2}\boldsymbol{\nabla}^2 + \hat{v}_{\mathrm{ext}}(\mathbf{r}) + \hat{v}(\mathbf{r}) + \hat{v}_x\right]\psi_n = \varepsilon_n\psi_n. \tag{2}$$

Here, $\hat{v}_{\mathrm{ext}}(\mathbf{r})$ is the external potential, i.e., the nuclear electron attraction. $\hat{v}(\mathbf{r})$ is the Coulomb potential and $\hat{v}_x$ the Hartree-Fock exchange, both caused by the electron-electron interaction.

The basic idea of the CIS approach is to use Slater determinants for the description of excited states, which are derived from the HF ground-state determinant by exciting an α electron from an occupied MO a to an unoccupied MO r (Ψ_a^r), or by exciting a β electron ($\Psi_{\bar{a}}^{\bar{r}}$), respectively. These singly excited Slater determinants are not pure spin states, but they can be combined to give either pure triplet or singlet states. Since we are only interested in the singlet excited-state manifold, we use the so-called singlet configuration state functions (CSFs),[26]

$${}^1\Psi_a^r = \frac{1}{\sqrt{2}}(\Psi_a^r + \Psi_{\bar{a}}^{\bar{r}}). \tag{3}$$

Note that sometimes ${}^1\Psi_a^r$ is given as $\frac{1}{\sqrt{2}}(\Psi_a^r - \Psi_{\bar{a}}^{\bar{r}})$. The sign depends on how one constructs the Slater determinants from a given set of MOs and in the following, different from prior publications, we will use the same method as in Ref. 25.

The field-free electronic Hamiltonian for a molecule with N electrons and N_A nuclei with charge Z_k,

$$\hat{H}_0 = -\frac{1}{2}\sum_{i=1}^{N}\boldsymbol{\nabla}_i^2 + \sum_{i=1}^{N}\sum_{j<i}^{N}\frac{1}{r_{ij}} - \sum_{k=1}^{N_A}\sum_{i=1}^{N}\frac{Z_k}{r_{ki}}, \tag{4}$$

can now be expressed in the basis of the restricted Hartree-Fock (RHF) ground-state Slater determinant and the singlet CSFs. This leads to the following matrix elements:[25]

$$\langle\Psi_0^{\mathrm{HF}}|\hat{H}_0|{}^1\Psi_a^r\rangle = 0, \tag{5}$$

$$\langle{}^1\Psi_a^r|\hat{H}_0 - E_{\mathrm{HF}}|{}^1\Psi_b^s\rangle = (\varepsilon_r - \varepsilon_a)\delta_{rs}\delta_{ab} - \langle\psi_r\psi_b|\psi_s\psi_a\rangle + 2\langle\psi_r\psi_b|\psi_a\psi_s\rangle. \tag{6}$$

We use the same notation for two-electron integrals as given in Ref. 25. Here, E_{HF} is the HF ground-state energy. By solving the following eigenvalue equation:

$$H^{\mathrm{CIS}}\mathbf{D}_i = E_i^{\mathrm{CIS}}\mathbf{D}_i, \tag{7}$$

we get the CIS excitation energies E_i^{CIS} and the CIS wave functions

$$\Psi_i = D_{0,i}\Psi_0^{\mathrm{HF}} + \sum_{a=L}^{N/2}\sum_{r=N/2+1}^{M} D_{a,i}^r\,{}^1\Psi_a^r. \tag{8}$$

L is the lowest occupied orbital and M the highest unoccupied orbital used to generate the excited determinants.

The perturbative corrections of the double-excited Slater determinants to these excitation energies are then calculated according to Ref. 22 as

$$E_i^{(\mathrm{D})} = -\frac{1}{4}\sum_{\mathrm{abrs}}\frac{(u_{\mathrm{ab},i}^{\mathrm{rs}})^2}{\Delta_{\mathrm{ab}}^{\mathrm{rs}} - E_i^{\mathrm{CIS}}} + \sum_{\mathrm{ar}} D_{\mathrm{a},i}^{\mathrm{r}}v_{\mathrm{a},i}^{\mathrm{r}}, \tag{9}$$

with

$$u^{\mathrm{rs}}_{\mathrm{ab},i} = \sum_{\mathrm{t}} [\langle \chi_{\mathrm{r}}\chi_{\mathrm{s}}||\chi_{\mathrm{t}}\chi_{\mathrm{b}}\rangle D^{\mathrm{t}}_{\mathrm{a},i} - \langle \chi_{\mathrm{r}}\chi_{\mathrm{s}}||\chi_{\mathrm{t}}\chi_{\mathrm{a}}\rangle D^{\mathrm{t}}_{\mathrm{b},i}] + \sum_{\mathrm{c}} [\langle \chi_{\mathrm{c}}\chi_{\mathrm{r}}||\chi_{\mathrm{a}}\chi_{\mathrm{b}}\rangle D^{\mathrm{s}}_{\mathrm{c},i} - \langle \chi_{\mathrm{c}}\chi_{\mathrm{s}}||\chi_{\mathrm{a}}\chi_{\mathrm{b}}\rangle D^{\mathrm{r}}_{\mathrm{c},i}], \tag{10}$$

$$v^{\mathrm{r}}_{\mathrm{a},i} = \frac{1}{2}\sum_{\mathrm{bcst}} \langle \chi_{\mathrm{b}}\chi_{\mathrm{c}}||\chi_{\mathrm{s}}\chi_{\mathrm{t}}\rangle (D^{\mathrm{s}}_{\mathrm{a},i} w^{\mathrm{tr}}_{\mathrm{bc}} + D^{\mathrm{r}}_{\mathrm{b},i} w^{\mathrm{ts}}_{\mathrm{ac}} + 2D^{\mathrm{s}}_{\mathrm{b},i} w^{\mathrm{rt}}_{\mathrm{ac}}), \tag{11}$$

$$w^{\mathrm{rs}}_{\mathrm{ab}} = -\frac{\langle \chi_{\mathrm{r}}\chi_{\mathrm{s}}||\chi_{\mathrm{a}}\chi_{\mathrm{b}}\rangle}{\Delta^{\mathrm{rs}}_{\mathrm{ab}}}, \tag{12}$$

$$\Delta^{\mathrm{rs}}_{\mathrm{ab}} = \varepsilon_{\mathrm{r}} + \varepsilon_{\mathrm{s}} - \varepsilon_{\mathrm{a}} - \varepsilon_{\mathrm{b}}. \tag{13}$$

We use the usual notation of $\langle \chi_{\mathrm{i}}\chi_{\mathrm{j}}||\chi_{\mathrm{k}}\chi_{\mathrm{l}}\rangle = \langle \chi_{\mathrm{i}}\chi_{\mathrm{j}}|\chi_{\mathrm{k}}\chi_{\mathrm{l}}\rangle - \langle \chi_{\mathrm{i}}\chi_{\mathrm{j}}|\chi_{\mathrm{l}}\chi_{\mathrm{k}}\rangle$ and χ_{i} denoting a spin orbital. The nonitalic indices correspond to spin orbitals, with a, b, and c indicating occupied HF MOs, and r, s, and t the unoccupied ones. (Indices of spatial orbitals are indicated by italic lower case letters.) The coefficients $D^{\mathrm{r}}_{\mathrm{a},i}$ for spin orbitals are easily obtained from the ones in the CSF basis as $D^{\mathrm{r}}_{\mathrm{a},i} = \frac{1}{\sqrt{2}} D^{r}_{a,i}$, if χ_{a} and χ_{r} have the same spin, and $D^{\mathrm{r}}_{\mathrm{a},i} = 0$, otherwise. The corrected excitation energies are then

$$E_i^{\mathrm{CIS(D)}} = E_i^{\mathrm{CIS}} + E_i^{(\mathrm{D})}. \tag{14}$$

B. Time propagation

The laser-driven many-electron dynamics is treated by solving the time-dependent Schrödinger equation

$$i\hbar \frac{\partial \Psi(t)}{\partial t} = \hat{H}(t)\Psi(t). \tag{15}$$

$\hat{H}(t)$ is a time-dependent electronic Hamiltonian, which includes the interaction with the laser field $\mathbf{F}(t)$ by means of the semiclassical dipole approximation

$$\hat{H}(t) = \hat{H}_0 - \hat{\boldsymbol{\mu}}\mathbf{F}(t), \tag{16}$$

where $\hat{\boldsymbol{\mu}} = -\sum_i^N \mathbf{r}_i + \sum_k^{N_A} Z_k \mathbf{R}_k$ is the molecular dipole operator. The applied (series of) laser pulses are chosen to be $\cos^2$-shaped,

$$\mathbf{F}(t) = \sum_n \mathbf{f}_n(t)\cos[\omega_n(t - t_{p,n}) + \Phi_n], \tag{17}$$

$$\mathbf{f}_n(t) = \begin{cases} \mathbf{f}_{0,n}\cos^2[\pi/(2\sigma_n)(t - t_{p,n})] & \text{if } |t - t_{p,n}| < \sigma_n \\ 0 \quad \text{else,} \end{cases} \tag{18}$$

where the index n indicates the number of the laser pulse. $\mathbf{f}_{0,n}$ gives the maximum amplitude and polarization, which is reached at $t_{p,n}$. ω_n, σ_n, and Φ_n determine the frequency, full width at half maximum (FWHM), and the phase of the nth laser pulse.

The time-dependent electronic wave function is expanded in the basis of the CIS states as

$$\Psi(t) = \sum_i C_i(t)\Psi_i, \tag{19}$$

where the initial wave function at $t=0$ is the RHF ground state Ψ_0^{HF}. For the time evolution of the coefficient vector $\mathbf{C}(t)$ during the laser pulses we use an operator splitting technique[27]

$$\mathbf{C}(t + \Delta t) = \left[\prod_{j=x,y,z} \mathbf{U}_j^{\dagger} e^{-iF_j(t)\tilde{\boldsymbol{\mu}}_j \Delta t}\mathbf{U}_j\right] e^{-i\tilde{\mathbf{H}}\Delta t}\mathbf{C}(t). \tag{20}$$

Here, $\tilde{\mathbf{H}}$ is the Hamilton matrix in the CIS eigenstate basis, which we assume to be diagonal, with the diagonal elements $\tilde{H}_{ii}$ being the CIS(D) excitation energies $E_i^{\mathrm{CIS(D)}}$. $\mathbf{U}_j$ $(j = x,y,z)$ are unitary matrices which transform from the CIS eigenstate basis to a basis in which the dipole matrices $\tilde{\boldsymbol{\mu}}_j$ are diagonal. When laser pulses are off the propagation becomes trival,

$$\Psi(t + \Delta t) = \sum_i C_i(t)\exp(-iE_i^{\mathrm{CIS(D)}}\Delta t)\Psi_i. \tag{21}$$

III. RESULTS

A. Static properties

The electronic structure of LiCN was calculated with a 6-31G* basis set.[28] The nuclear distances were set to their equilibrium values ($R_{\mathrm{Li-C}} = 3.683a_0$ and $R_{\mathrm{C-N}} = 2.168a_0$) determined by a geometry optimization for the linear molecule using the GAMESS (Ref. 29) program package. In the following we will use a coordinate system with the z axis as the symmetry axis of the molecule pointing from the Li atom to the N atom and the origin being the molecular center of mass. The one- and two-electron integrals in the atomic orbital (AO) basis were taken from the previous quantum chemistry calculation by GAMESS;[29] the rest of the program was written from scratch. As an internal consistency check of the code, the RHF wave function and HF ground-state properties were recalculated prior to the TD-CIS(D) computation. We include all molecular orbitals, except the three corresponding to the 1*s* atomic orbitals of Li, N, and C in the orbital space, which is used to generate the excited Slater determinants. By that choice, we have ten electrons in 42 MOs included in the CIS(D) calculation, leading to a total of 186 singlet CSFs including the ground-state determinant. All of these states, ranging up to about $5E_h$ above the ground state, were considered in this work.

Let us first discuss some of the results of the (stationary) CIS(D) calculations. For this purpose, the ten lowest-lying states are shown in the energy diagram of Fig. 1. Also indicated are permanent dipoles and transition dipole moments. The selected permanent dipoles and transition dipole moments are given in Table I. Since LiCN in the electronic ground state, characterized by the wave function Ψ_0, is a more or less ionic compound ($\mathrm{Li^+CN^-}$), the dipole moment along the z axis is comparatively large: $\mu_{0,0;z} = -3.708ea_0$ (−9.425 D). Because of the molecular symmetry (point group $C_{\infty v}$), the x and y components of the permanent dipole moment are identical to zero. The MP2 ground-state energy is $-100.0562E_h$, corresponding to a correlation energy of

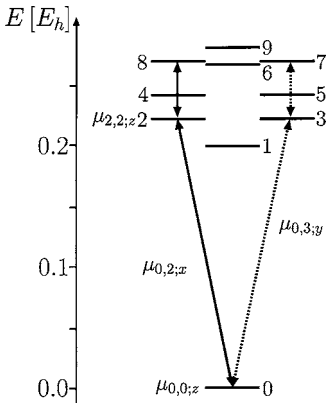

FIG. 1. The lowest ten electronic CIS(D) levels of LiCN together with selected transitions. The solid arrows indicate the transitions dominantly polarized along x and the dotted arrows the ones dominantly polarized along y. The values of the permanent dipole moments and the transition dipole moments are given in Table I.

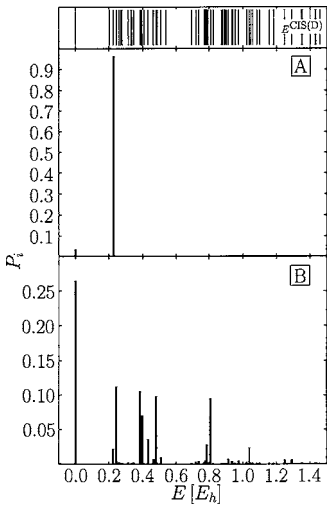

FIG. 2. Final population $P_i=|\langle\Psi_i|\Psi(t_f)\rangle|^2$ of the CIS(D) levels for two different π-pulse widths of (A) $2000\hbar/E_h$ and (B) $100\hbar/E_h$. Both pulses are x polarized and in resonance to the transition between the ground and the second excited state. The thin lines in the upper graph indicate the energies of the CIS(D) levels.

$0.2837E_h$ (7.72 eV). Above the ground state, there is a multitude of excited states. The first state, with wave function Ψ_1, is located at about $0.2E_h$ above the ground state and is uninteresting for our purposes below. Slightly above are two degenerate states Ψ_2 and Ψ_3. For these states the dipole moment is drastically different from the ground state, $\mu_{2,2;z}=2.795ea_0$ (7.105 D). The wave functions Ψ_2 and Ψ_3 are dominated by a singly excited CSF, which corresponds to a transfer of an electron from a π orbital localized at the CN group, to an antibonding σ^* orbital at the lithium atom. This means that these states describe mainly a covalent situation (LiCN), where both Li and the CN unit are neutral. Note that these states are easily optically accessible from the ground state, since the transition dipoles $\mu_{0,2;j}$ and $\mu_{0,3;j}$ are comparatively large. Specifically, from the dipole transition moments in Table I, one can see that such a transition can be either induced by a laser pulse polarized along x, leading to $\Psi_0\rightarrow\Psi_2$, or polarized along y, leading to $\Psi_0\rightarrow\Psi_3$. From Table I it is also evident that the eighth excited state Ψ_8 (which is degenerate with state Ψ_7) is useful, if one wants to control the charge distribution or dipole moment in the molecule; Ψ_8 is easily accessible from Ψ_2 (or Ψ_3) by large x- (or y-) polarized transition moments. The state Ψ_8 has a permanent dipole moment of $-1.1777ea_0$, which is right in between the values for the ionic and the covalent state. For this state the dominant excitation is from a π orbital localized at the CN group to a π^* orbital, which is located at both ends of the molecule. Therefore, one can view this state as one wherein about half an electron is transferred from the CN group to the Li atom. Apart from the states just discussed there are many others, single and degenerate ones, even in the low-energy regime, as indicated in Fig. 1 and in the upper panel of Fig. 2.

TABLE I. Selected permanent dipoles (a) and transition dipole moments (b) of LiCN. The corresponding transition moments in z are all zero. All values are given in ea_o.

(a)		(b)		
State	Dipole moment		$j=x$	$j=y$
$\mu_{0,0;z}$	−3.7082	$\mu_{0,2;j}$	+0.3084	+0.0095
$\mu_{2,2;z}$	+2.7952	$\mu_{0,3;j}$	+0.0095	−0.3084
$\mu_{3,3;z}$	+2.7952	$\mu_{2,8;j}$	−1.0333	+0.0325
$\mu_{8,8;z}$	−1.1777	$\mu_{3,7;j}$	−0.0325	−1.0333

B. Laser-driven dynamics

In the following we will focus on the dynamics of a laser-induced transition between the ground state, Ψ_0, and the second excited state, Ψ_2. For that purpose we apply x-polarized π pulses[27] with different widths σ. A π pulse induces a total population inversion in an ideal two-level system, assuming that the rotating wave approximation[30] is valid. This implies that we use a laser frequency resonant to the Ψ_0 to Ψ_2 transition, i.e., $\hbar\omega=0.2254E_h$ (6.1334 eV). For a $\cos^2$ envelope the condition for a π pulse is then given by $f_{0,x}\cdot\sigma=\hbar\pi/\mu_{0,2;x}$. Note that these approximations, i.e., the rotating wave approximation and the assumption of an ideal two-level system, are only used for the determination of the laser-pulse parameters. The actual time propagations are performed within the full CIS(D) state manifold without using the rotating wave approximation. Therefore, we get also some insight in the validity range of these approximations from our results, as discussed in the following. In all calculations presented here a time step of $\Delta t=0.01\hbar/E_h$ (0.24 as) is used, which gave converged results for all applied pulse intensities.

For the sake of simplicity we will not consider the small dipole transition moment along y for the Ψ_0 to Ψ_2 transition and the corresponding transition moment along x for the Ψ_0 to Ψ_3 transition in the following. Figures 2 and 3 display selected results for two different situations, namely, for a "long" π pulse with a width $\sigma=2000\hbar/E_h$ (48.4 fs) (A) and a "short" pulse of $\sigma=100\hbar/E_h$ (2.4 fs) (B). This corresponds to maximum light intensities of 9.13×10^{11} and 3.64×10^{14} W/cm^2, respectively.

Figure 2 shows the populations $P_i=|\langle\Psi_i|\Psi(t_f)\rangle|^2$ at the time t_f, when the laser pulse is over, of the CIS(D) levels

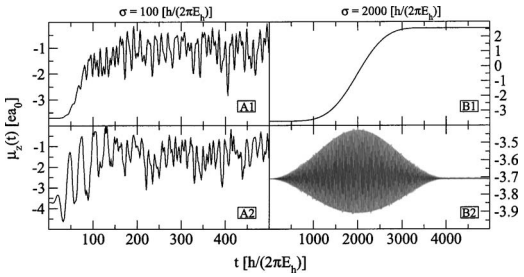

FIG. 3. Comparison of the z components of the time-dependent dipole moments for π pulses with a width of $100\hbar/E_h$ (left graphs, A1 and A2) and with a width of $2000\hbar/E_h$ (right graphs, B1 and B2). The pulses for A1 and B1 are x polarized, and the ones for A2 and B2 z polarized.

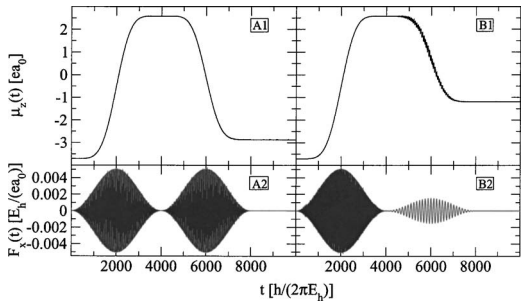

FIG. 4. Two control scenarios of the charge-transfer/dipole switching dynamics utilizing a sequence of two nonoverlapping, x-polarized π pulses. A1 shows the time-dependent dipole moment and A2 the corresponding laser field for a sequence $\Psi_0 \rightarrow \Psi_2 \rightarrow \Psi_0$. In B1 and B2 the complementary information is given for a scenario $\Psi_0 \rightarrow \Psi_2 \rightarrow \Psi_8$.

with up to an energy of about $1.5E_h$. As one can see in Fig. 2(A) the long pulse induces a nearly perfect population inversion between the ground state and the second excited state. For the shorter π pulse the situation is drastically different. Now, the wave function has contributions from many states—an electronic wave packet is formed instead of a single eigenstate. While the creation of a wave packet, which in few-state models is often artificially suppressed, offers interesting opportunities in general, in the present context it is unwanted for reasons to be outlined below. The final states populated from the ground state are fairly localized in energy windows which roughly correspond to multiples of the photon energy $n\hbar\omega$, keeping in mind that a 2.4-fs pulse has already a considerable energy width. Therefore, the excitation dynamics here is largely determined by resonant multiphoton excitations which are due to the higher intensity of the field. Also, after the short pulse we find population in states which have no transition dipole moments, from the ground state, i.e., these transitions are mediated by the polarizability and/or higher-order hyperpolarizabilities, which are also included in our model because we use the whole manifold of all excited CIS(D) states in the calculations.

These two effects of the short laser-pulse width and high intensity can be seen more clearly in Fig. 3. Shown here are the time-dependent dipole moments along z for four different situations. The curves in A1 and A2 are calculated with the short π pulse ($100\hbar/E_h$), while the ones in B1 and B2 for the long π pulse ($2000\hbar/E_h$). While for A1 and B1 the laser pulse is x polarized, A2 and B2 show results for a z-polarized laser. In B1 one can see a smooth transition from the permanent dipole moment of the ground state, $\mu_{0,0;z} \approx -3.7ea_0$, to that of the second excited state, $\mu_{2,2;z} \approx +2.8ea_0$, because here we are still in the limit where the molecule can be treated as an idealized two-level system. In B2 the same pulse is applied, but now polarized along z. Here, since the transition dipole $\mu_{0,2;z}$ is zero, the dipole moment along z has not changed after the pulse is over. Note, however, that during the pulse a dipole moment along z is induced, which follows nearly instantaneously the laser field and reflects the polarizability of the molecule. For the short pulses one can see in the x-polarized case (A1), that not a pure state is excited but a coherent superposition of excited states, i.e., an electron wave packet is being formed. As a result the z component of the molecular dipole behaves in an oscillatory manner and remains oscillatory even after the laser pulse is off. If nuclear motion is absent, the dipole moment corresponds to the time-dependent position expectation value of the electrons. Note that according to panel A2 of Fig. 3 even for the z-polarized case an electron wave packet is created, because now the intensity is high enough to create excited states through transitions which become allowed due to the polarizability or higher-order hyperpolarizabilities. So with the present method we can clearly distinguish the time scales in which the transition dynamics can be described by simplified models (e.g., dipole transitions in a two-level system), and those where one clearly needs explicitly time-resolved electron dynamics. It is also noted that with the present shape of the pulses, the pulse width cannot be chosen much shorter than $\sigma \approx 50$ fs, and still achieve a selective and complete state-to-state transition. However, this holds only for the chosen $\cos^2$-shaped pulses and it should be possible to further reduce this time limit by a more sophisticated choice of the laser pulse as discussed below (Sec. III C).

C. Controlling the charge transfer and dipole switching

After identifying the different time scales for the electron dynamics in our model molecule, we now want to discuss the possibility of controlling the charge-transfer/dipole switching dynamics by a series of short laser pulses. To begin with, we start with a series of π pulses derived from two-level situations, while in principle a more elaborate approach such as optimal control theory[31,32] may offer advantages. Hence, the only control parameters we are left with are the frequencies ω_n, the delay times $t_{p,n}$, and the phases Φ_n of the individual pulses.

Two rather simple scenarios to control the charge distribution and hence the dipole moment of the molecule are shown in Fig. 4. Here we utilize the findings from the previous section and use in both cases two x-polarized, nonoverlapping π pulses. Figure 4 A1 shows the time-dependent dipole moment along z and A2 the corresponding field for a sequence $\Psi_0 \rightarrow \Psi_2 \rightarrow \Psi_0$. Note that the system is nearly completely back in the ground state after this cycle. A reoptimization of pulses, which would improve the overlap between initial and final states, even further, was not attempted here but is expected to be easily possible.

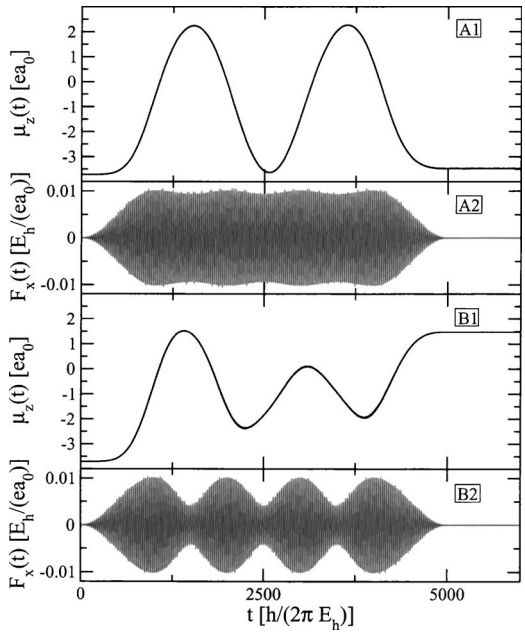

FIG. 5. Shown are the time-dependent dipole moments $\mu_z(t)$ (A1 and B1) induced by a sequence of four overlapping π pulses (A2 and B2) with a width of $\sigma=1000\hbar/E_h$ in resonance with the Ψ_0 to Ψ_2 transition. In the first case (A) the pulses interfere constructively, and in the second case (B) destructively.

The panels B1 and B2 of Fig. 4 show a similar situation, only here the second transition from the intermediate state Ψ_2 is to Ψ_8 rather than back to Ψ_0. As a consequence, the dipole switches between three well-defined values in this case, rather than two as in A1 and A2. In general, a multitude of reversible and reproducible dipole switching sequences is expected to be possible in a simple molecule by the use of a series of shaped, femtosecond laser pulses which lead to selective state-to-state transitions.

However, as stated above the second excited state of LiCN is repulsive with respect to the Li–C bond. Therefore, during a time scale of about 200 fs as shown in Fig. 4, the molecule might dissociate. One may overcome this problem by choosing a molecule with less dramatic differences in the potential-energy curves for ground and excited states. Another possibility is to speed up the switching process. This can be done by more sophisticated control strategies, but we will stick to π pulses for now. Figure 5 shows the time-dependent dipoles $\mu_z(t)$ (A1 and B1) and the electric fields (A2 and B2) for two alternative scenarios. In both cases a series of four overlapping π pulses (A2 and B2) has been used. All pulses have the same width of $\sigma=1000\hbar/E_h$, and are in resonance with the Ψ_0 to Ψ_2 transition. In the first case (A), the pulses interfere constructively, while in the second case (B) the phases are in such a way that destructive interference occurs. For the first case (A) it is then possible to switch the dipole moment four times in roughly 120 fs and still end up in a pure state, i.e., without creating an electronic wave packet. The second sequence switches the orientation of the dipole moment even five times, though not completely, but ending mainly in the excited state. The example shows that fast switching even of multistate systems is possible in very short times, and further, that the phase relation between individual pulses is of great importance.

IV. CONCLUSIONS AND OUTLOOK

We applied the TD-CIS(D) method to the laser-driven charge transfer and the accompanying dipole switching in the LiCN molecule, which serves as a simple model system. Various effects can be described in this *ab initio* model, such as state-to-state transitions, the creation of electron wave packets, multiphoton transitions, and effects of the polarizability and higher-order hyperpolarizabilities. The present method can be improved systematically towards the exact, full CI solution by including higher excited Slater determinants explicitly, e.g., the configuration-interaction singles and doubles (CISD). Another possibility is to include higher excited determinants also by perturbation theory configuration-interaction singles (doubles, triples, and quadruples) [CIS(DTQ)] as recently done in Ref. 33.

For the described charge-transfer dynamics we demonstrated a simple control scenario utilizing π pulses. For future work we want to implement a more sophisticated approach such as the optimal control theory.[31,32] It is also possible to treat larger molecules, which offer a more realistic route to practical applications, for example, by fixating these molecules either on a surface or inside a break junction.

ACKNOWLEDGMENTS

We thank E. K. U. Gross for suggesting this molecule and gratefully acknowledge support on this work by the Deutsche Forschungsgemeinschaft through Project No. Sa 547/6 (SPP-1145).

[1] *Molecular Electronics*, edited by J. Jortner and M. Ratner (Blackwell, Oxford, 1997).
[2] A. Nitzan, Annu. Rev. Phys. Chem. **52**, 681 (2001).
[3] J. Jortner, Philos. Trans. R. Soc. London, Ser. A **356**, 477 (1998).
[4] J. Breidbach and L. S. Cederbaum, J. Chem. Phys. **118**, 3983 (2003).
[5] M. Drescher, M. Hentschel, R. Kienberger *et al.*, Nature (London) **419**, 803 (2002).
[6] G. G. Paulus, F. Lindner, H. Walther, A. Baltuška, E. Goulielmakis, M. Lezius, and F. Krausz, Phys. Rev. Lett. **91**, 253004 (2003).
[7] X. Liu, H. Rottke, E. Eremina, Phys. Rev. Lett. **93**, 263001 (2004).
[8] K. O'Keeffe, P. Jöchl, H. Drexel, V. Grill, F. Krausz, and M. Lezius, Appl. Phys. B: Lasers Opt. **78**, 583 (2004).
[9] K. Harumiya, I. Kawata, H. Kono, and Y. Fujimura, J. Chem. Phys. **113**, 8953 (2000).
[10] J. Colgan, S. D. Loch, M. S. Pindzola, C. Ballance, and D. C. Griffin, Phys. Rev. A **68**, 032712 (2003).
[11] K. C. Kulander, Phys. Rev. A **36**, 2726 (1987).
[12] E. Runge and E. K. U. Gross, Phys. Rev. Lett. **52**, 997 (1984).
[13] F. Calvayrac, P.-G. Reinhard, E. Suraud, and C. A. Ullrich, Phys. Rep. **337**, 493 (2000).
[14] A. Castro, M. A. L. Marques, J. A. Alonso, G. F. Bertsch, and A. Rubio, Eur. Phys. J. D **28**, 211 (2004).
[15] T. Klamroth, Phys. Rev. B **68**, 245421 (2003).
[16] C. Huber and T. Klamroth, Appl. Phys. A: Mater. Sci. Process. **87**, 93 (2005).
[17] D. Hegarty and M. A. Robb, Mol. Phys. **38**, 1795 (1979).
[18] J. Zanghellini, M. Kitzler, C. Fabian, T. Brabec, and A. Scrinzi, Laser Phys. **13**, 1064 (2003).
[19] T. Kato and H. Kono, Chem. Phys. Lett. **392**, 533 (2004).
[20] M. Nest, T. Klamroth, and P. Saalfrank, J. Chem. Phys. **122**, 124102 (2005).
[21] M. H. Beck, A. Jäckle, G. A. Worth, and H.-D. Meyer, Phys. Rep. **324**, 1 (2000).
[22] M. Head-Gordon, R. J. Rico, M. Oumi, and T. J. Lee, Chem. Phys. Lett. **219**, 21 (1994).

[23] M. Head-Gordon, D. Maurice, and M. Oumi, Chem. Phys. Lett. **246**, 114 (1995).
[24] J. B. Foresman, M. Head-Gordon, J. A. Pople, and M. J. Frisch, J. Phys. Chem. **96**, 135 (1992).
[25] A. Szabo and N. S. Ostlund, *Modern Quantum Chemistry*, 1st (revised) ed. (McGraw-Hill, New York, 1989).
[26] R. Paunz, *Spin Eigenfunctions* (Plenum, New York, 1979).
[27] A. D. Bandrauk, E. Aubanel, and S. Chelkowski, in *Femtosecond Chemistry*, edited by J. Manz and L. Wöste (Verlag Chemie, New York, 1995), Vol. 2, Chap. 25, p. 731.
[28] P. C. Hariharan and J. A. Pople, Theor. Chim. Acta **28**, 213 (1973).
[29] M. W. Schmidt, K. K. Baldridge, J. A. Boatz *et al.*, J. Comput. Chem. **13**, 1347 (1993).
[30] I. Rabi, Phys. Rev. **51**, 652 (1937).
[31] S. Shi, A. Woody, and H. Rabitz, J. Chem. Phys. **88**, 6870 (1988).
[32] R. Kosloff, S. A. Rice, P. Gaspard, S. Tersigni, and D. J. Tannor, Chem. Phys. **139**, 201 (1989).
[33] S. Hirata, J. Chem. Phys. **122**, 094105 (2005).